Theoretical and Computational Acoustics
D. Lee, Y-H Pao, M.H. Schultz, and Y-C Teng (Editors)

On the Stability of a Finite, Baffled Elastic Plate in Mean Flow

Sean F. Wu and Jinshuo Zhu
Department of Mechanical Engineering
Wayne State University, Detroit, MI 48202

ABSTRACT

This paper presents a stability analysis of a finite, elastic plate in the presence of mean flow. The edges of the plate are assumed to be clamped to an infinite, rigid baffle. The effect of structural nonlinearities induced by inplane forces and shearing forces due to stretching of plate bending motion is considered. The plate flexural displacement is determined by the Galerkin's method. The critical mean flow speeds at which local instabilities may occur are solved analytically. The mechanisms that trigger the onset of the local instabilities are uncovered. The effect of mean flow and that of structural nonlinearities on the plate stabilities are examined. Finally, numerical examples of transition from stable to locally unstable vibration as the mean flow speed increases are demonstrated. Numerical results show that while the overall amplitude of the plate flexural displacement may be bounded when the mean flow speed exceeds the critical ones, plate vibration may be locally unstable, jumping from one equilibrium position to another. This jumping may be completely random, and plate vibration may seem to be totally chaotic.

1. INTRODUCTION

There have been many research activities on the stability analysis of an elastic plate in subsonic and supersonic flows.[1 – 6] Most of the studies in subsonic mean flow, however, are confined to a linear system whose response may grow unboundedly in time, known as absolute instability, when the mean flow speed exceeds certain critical value. The first numerical example of absolute instability for an infinite plate was shown by Brazier-Smith and Scott.[7] Crighton and Oswell[8] proved analytically the existence of absolute instability for an infinite plate in mean flow. The critical mean flow speed beyond which absolute instability would occur was shown[8] to depend on the fluid/structure densities' and compressional wave speeds' ratios only. Consequently, absolute instability may occur for an infinite steel plate in water when the mean flow speed exceeds 14.9 m/s, or for the same plate in the air when the mean flow speed exceeds only 0.02 m/s, disregard the thickness of the plate. These are quite startling results. Yet, the mechanisms that trigger absolute instability are never explained.

Clearly, in reality there are no infinite plates and the amplitudes of plate vibration will never grow unboundedly. Hence in this paper we consider a finite, elastic plate. In particular, we include the effect of structural nonlinearities induced by inplane forces and shearing forces due to stretching of the plate bending motion. The objective is to gain a better understanding of the physics involved in this complex fluid-structure interaction. Specifically, we want to know how and when plate flexural vibration may become unstable in the presence of mean flow, how the plate aspect ratio and thickness may affect its instability, and finally, what the role of the viscous damping ratio may play in the plate stability.

Section 2 of this paper presents the equation governing the plate flexural vibration. The acoustic pressure acting on the plate surface is determined by a three-dimensional temporal Green's function. The plate flexural displacement is obtained by the Galerkin's method in section 3. The critical mean flow speeds at which local instabilities may occur are solved analytically using the Routh's stability criterion in section 4. The effect of mean flow speeds and that of structural nonlinearities on local instabilities are examined at each equilibrium position for a specific example that involves two longitudinal and one lateral modes. Numerical examples that indicate transition from stable to unstable vibration as the mean flow speed increases are demonstrated in section 5. Conclusions are drawn in section 6.

2. PLATE FLEXURAL VIBRATION EQUATION

Consider a rectangular plate of length L and width b that is clamped to an infinite, rigid baffle. The plate is in contact with some fluid on one side ($z > 0$), and vacuum on the other side. The fluid is assumed to move at a constant, uniform speed in the $x > 0$ direction.

In deriving the equation governing the plate flexural vibration, we take into account the effect of viscous damping and that of structural nonlinearities induced by inplane forces and shearing forces due to stretching of plate bending motion. Since we are interested in plate free vibrational motion, the only external forcing will be the radiated acoustic pressure that acts back to the plate surface. Accordingly, the plate flexural vibration equation can be written as[9]

$$\left(D\nabla^4 + d\frac{\partial}{\partial t} + \rho_p h\frac{\partial^2}{\partial t^2} - N_x\frac{\partial^2}{\partial x^2} - N_y\frac{\partial^2}{\partial y^2} - 2N_{xy}\frac{\partial^2}{\partial x \partial y}\right) w(x,y,t) = -p(x,y,0,t), \quad (1)$$

where w is the plate flexural deflection, $D = Eh^3/12/(1-\nu^2)$, is the plate bending rigidity, h, ρ_p, E, ν, and d are the plate's thickness, density, Young's modulus, Poisson ratio, and viscous damping coefficient, respectively, N_x N_y, and N_{xy} are inplane forces and shearing forces due to stretching of plate bending motion[9]

$$N_x = \frac{Eh}{2L}\int_0^L \left[\frac{\partial w(x,y,t)}{\partial x}\right]^2 dx, \tag{2a}$$

$$N_y = \frac{Eh}{2b}\int_0^b \left[\frac{\partial w(x,y,t)}{\partial y}\right]^2 dy, \tag{2b}$$

$$N_{xy} = \frac{Eh}{2bL}\int_0^b\int_0^L \frac{\partial w(x,y,t)}{\partial x}\frac{\partial w(x,y,t)}{\partial y} dxdy, \tag{2c}$$

The surface pressure on the right side of Eq.(1) is related the velocity potential function ϕ[10]

$$p(x,y,z,t) = -\rho_0\left[\frac{\partial}{\partial t} + U\frac{\partial}{\partial x}\right]\phi(x,y,z,t), \tag{3}$$

where ρ_0 is the density of fluid. The potential function can be written as[11, 12]

$$\phi(x,y,z,t) = \int_0^L\int_0^b \left[G_0(\vec{r}|\vec{r}_o)\left(\frac{\partial}{\partial \tau} + U\frac{\partial}{\partial x_o}\right)w(x_o,y_o,\tau)\right]_\tau dx_o dy_o, \tag{4}$$

where G_0 is defined as

$$G_0(\vec{r}|\vec{r}_o) = -\frac{1}{2\pi\sqrt{1-M^2}\sqrt{R^2+u^2}}, \tag{5}$$

where $R^2 = (y-y_o)^2 + z^2$, $u = (x-x_o)(1-M^2)^{-1/2}$, M is the Mach number of the mean flow speed, the symbol $[\ \ ]_\tau$ in Eq. (4) implies that the quantities inside the square brackets are to be evaluated at the retarded time $\tau = t - \Delta t$, here Δt is given by

$$\Delta t = \frac{\sqrt{R^2+u^2} - Mu}{c\sqrt{1-M^2}}. \tag{6}$$

For a heavy fluid medium such as water and for a small value of R compared with the wavelength of the emitted sound, the time delay Δt can be omitted to in order to simplify the numerical computations.

Substituting Eq. (4) into (3) yields,

$$p(x,y,0,t) = -\rho_0\left(\frac{\partial}{\partial t} + U\frac{\partial}{\partial x}\right)\int_0^L\int_0^b \left[G_0(\vec{r}|\vec{r}_o)\left(\frac{\partial}{\partial \tau} + U\frac{\partial}{\partial x_o}\right)w(x_o,y_o,\tau)\right]_\tau dx_o dy_o. \tag{7}$$

To alleviate the singularity difficulty caused by taking the derivative of G_0 with respect to x in Eq. (7), we replace $\partial G_0(\vec{r}|\vec{r}_o)/\partial x$ by $-\partial G_0(\vec{r}|\vec{r}_o)/\partial x_o$, and use the chain rule to transfer the derivative with respect to x_o to $w(x_o, y_o, \tau)$. Further, for a clamped plate, the displacement and slope at the edges are identically zero. Thus, without regard to the time delay we can rewrite Eq. (7) as

$$p(x,y,0,t) = -\rho_0 \int_0^L \int_0^b G_0(\vec{r}|\vec{r}_o) \left(\frac{\partial}{\partial t} + U \frac{\partial}{\partial x_0} \right)^2 w(x_o, y_o, t) dx_o dy_o. \quad (8)$$

3. PLATE FLEXURAL DISPLACEMENT

Substituting Eq. (8) into (1) yields a differential, integral equation that governs the plate flexural vibrational motion. Because of the complexities involved in this equation, analytic solution cannot be obtained. Hence, we use the Galerkin's method to obtain an approximate solution. Namely, we expand the plate flexural displacement in terms of the normal modes in that satisfy the prescribed boundary conditions

$$w(x,y,t) = \{W(x)\}^{\mathrm{T}}[C(t)]\{W(y)\}, \quad (9)$$

where $\{W(x)\}$ and $\{W(y)\}$ represent N longitudinal and M lateral normal modes, respectively, a superscription T in Eq. (9) indicates a transposition, and $[C(t)]$ stand for the amplitudes of coupling between the lateral and the longitudinal modes.

For the clamped boundary conditions, $W_k(x)$ and $W_i(y)$ are given by

$$W_k(x) = \sigma_k \left[sin\left(\frac{\lambda_k x}{L}\right) - sinh\left(\frac{\lambda_k x}{L}\right) \right] + \left[cos\left(\frac{\lambda_k x}{L}\right) - cosh\left(\frac{\lambda_k x}{L}\right) \right], \quad (10a)$$

$$W_i(y) = \sigma_i \left[sin\left(\frac{\lambda_i x}{b}\right) - sinh\left(\frac{\lambda_i y}{b}\right) \right] + \left[cos\left(\frac{\lambda_i y}{b}\right) - cosh\left(\frac{\lambda_i y}{b}\right) \right], \quad (10b)$$

where σ_i represents the ith modal ratio

$$\sigma_i = \frac{\sin\lambda_i + \sinh\lambda_i}{\cos\lambda_i - \cosh\lambda_i}, \quad (11)$$

where λ_i is the ith eigenvalue determined by

$$\cos\lambda_i \cosh\lambda_i = 1. \quad (12)$$

Note that the normal modes $\{W(x)\}$ and $\{W(y)\}$ are orthogonal to each other

$$\int_0^L W_k(x) W_l(x) dx = \begin{cases} L & \text{for} \quad k = l; \\ 0 & \text{for} \quad k \neq l. \end{cases} \quad (13a)$$

$$\int_0^b W_i(y)W_j(y)dy = \begin{cases} b & \text{for } i = j; \\ 0 & \text{for } i \neq j. \end{cases} \tag{13a}$$

However, the products of $\{W(x)\}$ and its derivatives are not necessarily orthogonal.

Substituting Eqs. (10) into (1), multiplying the resultant equation by $\{W(x)\}$, integrating over x from 0 to L, and then multiplying by $\{W(y)\}$ and integrating over y from 0 to b, we obtain

$$[\Phi][\ddot{C}(\bar{t})] + [\Psi][\dot{C}(\bar{t})] + [\chi][C(\bar{t})] - [\Xi][C(\bar{t})] = 0, \tag{14}$$

where $[\Phi]$, $[\Psi]$, and $[\chi]$ represent the effects of mass, damping, stiffness per unit area of the plate, respectively, and $[\Xi]$ stand for the effect of structural nonlinearities and contain quadratic powers of the unknown coefficients $[C(\bar{t})]$. The elements of these matrices can be written in the following general forms

$$\Phi_{klij} = \delta_{ik}\delta_{jl} + \frac{\eta\mu}{2\pi\sqrt{1-M^2}}\Theta^{(0)}_{klij}, \tag{15a}$$

$$\Psi_{klij} = \xi\delta_{ik}\delta_{jl} + \frac{\eta\zeta\sqrt{\mu}}{\pi\sqrt{1-M^2}}\Theta^{(1)}_{klij}, \tag{15b}$$

$$\chi_{klij} = \left[\lambda_i^4 + \frac{\lambda_j^4}{\eta^4}\right]\delta_{ik}\delta_{jl} + \frac{2}{\eta^2}\theta_{ik}\theta_{jl} + \frac{\eta\zeta^2}{2\pi\sqrt{1-M^2}}\Theta^{(2)}_{klij}, \tag{15c}$$

$$\Xi_{klij} = 6(1-\nu^2)\bar{C}_{pq}(\bar{t})\bar{C}_{rs}(\bar{t})\left[\theta_{pr}\theta_{ik}\beta_{jlqs} + \theta_{qs}\theta_{jl}\beta_{ikpr} - \gamma_{pr}\gamma_{sq}\gamma_{ik}\gamma_{jl}\right], \tag{15d}$$

where δ_{ij} represent the Kronecker delta.

Note that the second term on the right side of Eq. (15a) represents the effect of added mass due to acoustic radiation; the second term on the right side of Eq. (15b) represents the effect of added damping induced by acoustic radiation in the presence of mean flow; the second and the third terms on the right side of Eq. (15c) represent the effect of added stiffness due to acoustic radiation and mean flow, respectively; and the terms on the right side of Eq. (15d) represent the effect of added stiffness due to structural nonlinearities.

In Eqs. (15), the subscripts i, k, p, $r = 1, 2, \cdots N$ and j, l, q, $s = 1, 2, \cdots M$, and a bar implies a dimensionless quantity

$$\bar{C}_{ij} = \frac{C_{ij}}{h}, \quad \bar{t} = t\sqrt{\frac{D}{\rho_p h L^4}}, \quad (\bar{x}, \bar{x}_o) = \frac{(x, x_o)}{L}, \quad (\bar{y}, \bar{y}_o) = \frac{(y, y_o)}{b}, \tag{16a}$$

and the parameters η, ξ, μ, and ζ in Eqs. (15) are given by

$$\eta = \frac{b}{L}, \qquad \xi = d\sqrt{\frac{L^4}{D\rho_p h}}, \qquad \mu = \frac{\rho_0 L}{\rho_p h}, \qquad \zeta = U\sqrt{\frac{\rho_0 L^3}{D}}. \tag{16b}$$

Physically, the quantities η, ξ, μ, and ζ reflect the effects of the plate aspect ratio, damping ratio, fluid/structure density ratio, and dimensionless mean flow speed, respectively.

The quantities θ, γ, β, and Θ in Eqs. (15) are defined as follows

$$\theta_{ik} = \int_0^1 \frac{\partial^2 W_i(\bar{x})}{\partial \bar{x}^2} W_i(\bar{x}) W_k(\bar{x}) d\bar{x}, \tag{17a}$$

$$\gamma_{ik} = \int_0^1 \frac{\partial W_i(\bar{x})}{\partial \bar{x}} W_k(\bar{x}) d\bar{x}, \tag{17b}$$

$$\beta_{jlqs} = \int_0^1 W_j(\bar{y}) W_l(\bar{y}) W_q(\bar{y}) W_s(\bar{y}) d\bar{y}, \tag{17c}$$

$$\Theta_{klij}^{(v)} = \int_0^1\int_0^1 W_k(\bar{x}) W_l(\bar{y}) d\bar{x} d\bar{y} \int_0^1\int_0^1 \frac{\frac{\partial^v}{\partial x_0^v} W_i(\bar{x}_o) W_j(\bar{y}_o)}{\sqrt{(\bar{x}-\bar{x}_o)^2 + \eta^2(1-M^2)(\bar{y}-\bar{y}_o)^2}} d\bar{x}_o d\bar{y}_o. \tag{17d}$$

4. STABILITY ANALYSIS

In this section we present a stability analysis of the system described by the matrix equation (14). For simplicity, let us consider only one lateral and two longitudinal modes. Thus, Eq. (14) reduces to a set of two simultaneous nonlinear ordinary differential equations (NODEs),

$$\begin{aligned}\left(1 + \frac{\eta\mu}{2\pi}\Theta_{1111}^{(0)}\right)\ddot{\bar{C}}_{11}(\bar{t}) + \xi\dot{\bar{C}}_{11}(\bar{t}) + \frac{\eta\zeta\sqrt{\mu}}{\pi}\Theta_{1121}^{(1)}\dot{\bar{C}}_{21}(\bar{t}) \\ + \left(\lambda_1^4 + 2\frac{\theta_{11}^2}{\eta^2} + \frac{\lambda_1^4}{\eta^4} + \frac{\eta\zeta^2}{2\pi}\Theta_{1111}^{(2)}\right)\bar{C}_{11}(\bar{t}) \\ + 6\left(1-\nu^2\right)\left(\theta_{11}\bar{C}_{11}^2 + \theta_{22}\bar{C}_{22}^2\right)\beta_{1111}\theta_{11}\bar{C}_{22} = 0,\end{aligned} \tag{18a}$$

$$\begin{aligned}\left(1 + \frac{\eta\mu}{2\pi}\Theta_{2121}^{(0)}\right)\ddot{\bar{C}}_{21}(\bar{t}) + \xi\dot{\bar{C}}_{21}(\bar{t}) - \frac{\eta\zeta\sqrt{\mu}}{\pi}\Theta_{1121}^{(1)}\dot{\bar{C}}_{11}(\bar{t}) \\ + \left(\lambda_2^4 + 2\frac{\theta_{11}\theta_{22}}{\eta^2} + \frac{\lambda_1^4}{\eta^4} + \frac{\eta\zeta^2}{2\pi}\Theta_{2121}^{(2)}\right)\bar{C}_{21}(\bar{t}) \\ + 6\left(1-\nu^2\right)\left(\theta_{11}\bar{C}_{11}^2 + \theta_{22}\bar{C}_{22}^2\right)\beta_{1111}\theta_{22}\bar{C}_{22} = 0.\end{aligned} \tag{18b}$$

Equations (18) can be further simplified by introducing the following dimensionless parameters

$$\alpha_{01} = 1 + \frac{\eta\mu}{2\pi}\Theta_{1111}^{(0)}, \tag{19a}$$

$$\alpha_{02} = 1 + \frac{\eta\mu}{2\pi}\Theta_{2121}^{(0)}, \tag{19b}$$

$$\alpha_1 = \lambda_1^4 + 2\frac{\theta_{11}^2}{\eta^2} + \frac{\lambda_1^4}{\eta^4} + \frac{\eta\zeta^2}{2\pi}\Theta_{1111}^{(2)}, \tag{19c}$$

$$\alpha_2 = \lambda_2^4 + 2\frac{\theta_{11}\theta_{22}}{\eta^2} + \frac{\lambda_1^4}{\eta^4} + \frac{\eta\zeta^2}{2\pi}\Theta_{2121}^{(2)}, \tag{19d}$$

$$\alpha_3 = \frac{\eta\zeta\sqrt{\mu}}{\pi}\Theta_{1121}^{(1)}, \tag{19e}$$

$$\alpha_4 = 6\left(1-\nu^2\right)\left(1+\frac{1}{\eta^4}\right)\beta_{1111}, \tag{19f}$$

$$\alpha_5 = 6\left(1-\nu^2\right)\left(\beta_{1111}\theta_{11}\theta_{22} + \frac{3}{\eta^4}\beta_{1122}\theta_{11}^2\right), \tag{19g}$$

$$\alpha_6 = 6\left(1-\nu^2\right)\left(\beta_{1111}\theta_{22}^2 + \frac{1}{\eta^4}\beta_{2222}\theta_{22}^2\right), \tag{19h}$$

and new variables

$$Y_1 = \bar{C}_{11}(\bar{t}), \tag{20a}$$

$$Y_2 = \dot{\bar{C}}_{11}(\bar{t}), \tag{20b}$$

$$Y_3 = \bar{C}_{21}(\bar{t}), \tag{20c}$$

$$Y_4 = \dot{\bar{C}}_{21}(\bar{t}). \tag{20e}$$

Substituting Eqs. (19) and (20) into (18) yields a set of four first-order NODEs,

$$\dot{Y}_1 = Y_2, \tag{21a}$$

$$\dot{Y}_2 = -\frac{\alpha_1}{\alpha_{01}}Y_1 - \frac{\xi}{\alpha_{01}}Y_2 - \frac{\alpha_3}{\alpha_{01}}Y_4 - \frac{\alpha_4}{\alpha_{01}}Y_1^3 - \frac{\alpha_5}{\alpha_{01}}Y_1Y_3^2, \tag{21b}$$

$$\dot{Y}_3 = Y_4, \tag{21c}$$

$$\dot{Y}_4 = -\frac{\alpha_2}{\alpha_{02}}Y_3 - \frac{\xi}{\alpha_{02}}Y_4 + \frac{\alpha_3}{\alpha_{02}}Y_2 - \frac{\alpha_5}{\alpha_{02}}Y_1^2Y_3 - \frac{\alpha_6}{\alpha_{02}}Y_3^3. \tag{21d}$$

Equation (21) allows us to use the stability theory[13] to examine the local instabilities around the fixed points or equilibrium positions determined by setting the right side of Eq. (21) to zero.

$$Y_2 = 0, \tag{22a}$$

$$\left(\alpha_1 + \alpha_4 Y_1^2 + \alpha_5 Y_3^2\right) Y_1 = 0, \tag{22b}$$

$$Y_4 = 0, \tag{22c}$$

$$\left(\alpha_2 + \alpha_5 Y_1^2 + \alpha_6 Y_3^2\right) Y_3 = 0. \tag{22d}$$

The possible solutions to Eqs. (22) are given by

$$\tilde{Y}_1 = \tilde{Y}_2 = \tilde{Y}_3 = \tilde{Y}_4 = 0, \tag{23a}$$

$$\tilde{Y}_2 = \tilde{Y}_3 = \tilde{Y}_4 = 0, \qquad \tilde{Y}_1 = \pm\sqrt{-\frac{\alpha_1}{\alpha_4}}, \tag{23b}$$

$$\tilde{Y}_1 = \tilde{Y}_2 = \tilde{Y}_4 = 0, \qquad \tilde{Y}_3 = \pm\sqrt{-\frac{\alpha_2}{\alpha_6}}, \tag{23c}$$

$$\tilde{Y}_2 = \tilde{Y}_4 = 0, \qquad \tilde{Y}_1 = \pm\sqrt{\frac{\alpha_2\alpha_5 - \alpha_1\alpha_6}{\alpha_4\alpha_6 - \alpha_5^2}}, \qquad \tilde{Y}_3 = \pm\sqrt{\frac{\alpha_1\alpha_5 - \alpha_2\alpha_4}{\alpha_4\alpha_6 - \alpha_5^2}}, \tag{23d}$$

where the symbol $\tilde{Y}$ implies a fixed point or an equilibrium position. Note that solutions given by Eqs. (23) must be real in order for the equilibrium position to be meaningful.

Clearly, the equilibrium position given by Eq. (23a) is the plate undeformed flat position, and the rest are induced by structural nonlinearities. Equations (23) indicate that the plate may vibrate either around its flat equilibrium or around other equilibrium positions.

The stabilities of the plate can now be examined at the equilibrium positions given by Eq. (23). Taking the derivative of Eq. (22) with respect to time, we obtain

$$\mathcal{J}(Y)\{\dot{Y}\} = 0, \tag{24}$$

where $\mathcal{J}(Y)$ is the Jacobian matrix given by

$$\mathcal{J}(Y) = \begin{bmatrix} 0 & 1 & 0 & 0 \\ -\frac{\alpha_1+3\alpha_4Y_1^2+\alpha_5Y_3^2}{\alpha_{01}} & -\frac{\xi}{\alpha_1} & -\frac{2\alpha_5Y_1Y_3}{\alpha_{01}} & -\frac{\alpha_3}{\alpha_{01}} \\ 0 & 0 & 0 & 1 \\ -\frac{2\alpha_5Y_1Y_3}{\alpha_{02}} & \frac{\alpha_3}{\alpha_{02}} & -\frac{\alpha_2+\alpha_5Y_1^2+3\alpha_6Y_3^2}{\alpha_{02}} & -\frac{\xi}{\alpha_{02}} \end{bmatrix}. \tag{25}$$

Next, we assume a form of solution to Eq. (24)

$$\{Y\} = \{|Y|\}e^{\Lambda\bar{t}}, \tag{26}$$

where Λ represents the eigenvalue of the system and $\{|Y|\}$ stands for the amplitude of $\{Y\}$.

Substituting Eq. (26) into (24) leads to the characteristic equation

$$\sum_{n=0}^{4} \Omega_n\Lambda^n = 0, \tag{27}$$

where Ω_n are given by

$$\Omega_0 = \Gamma_1\Gamma_2 - 4\alpha_5^2 Y_1^2 Y_3^2, \quad (28a)$$
$$\Omega_1 = \xi(\Gamma_1 + \Gamma_2), \quad (28b)$$
$$\Omega_2 = \xi^2 + \alpha_3^2 + \alpha_{01}\Gamma_2 + \alpha_{02}\Gamma_1, \quad (28c)$$
$$\Omega_3 = \xi(\alpha_{01} + \alpha_{02}), \quad (28d)$$
$$\Omega_4 = \alpha_{01}\alpha_{02}, \quad (28e)$$

where

$$\Gamma_1 = \alpha_1 + 3\alpha_4 Y_1^2 + \alpha_5 Y_3^2, \quad (29a)$$
$$\Gamma_2 = \alpha_2 + \alpha_5 Y_1^2 + 3\alpha_6 Y_3^2. \quad (29b)$$

The stability theorem for linear systems[14] states that a system is stable if and only of the roots of the characteristics equation all lie in the left-half Λ plane, excluding the imaginary axis. This theorem is also applicable for the system under consideration. One way of determining whether the roots of the polynomial equation (27) all lie in the left-half Λ plane without actually solving for them is through the Routh's algorithm,[14] which yields the following inequalities

$$\Omega_0 > 0, \quad \Omega_1 > 0, \quad \Omega_2 > 0, \quad \Omega_3 > 0, \quad \Omega_4 > 0, \quad (30a)$$
$$\Omega_2\Omega_3 - \Omega_1\Omega_4 > 0, \quad (30b)$$
$$\Omega_1(\Omega_2 - \Omega_1\Omega_4) - \Omega_0\Omega_3^2 > 0. \quad (30c)$$

Substituting Eqs. (28) into (30) then leads to the following conditions

$$\xi > 0, \quad \alpha_{01} > 0, \quad \alpha_{02} > 0, \quad \Gamma_1 > 0, \quad \Gamma_2 > 0, \quad (31)$$

which must all be satisfied in order for the system defined by Eq. (21) to be stable.

Equation (31) may shed some light on the mechanisms involved in the local instabilities of a fluid-loaded plate in mean flow.

- The first inequality in Eq. (31) requires that the damping ratio ξ be positive. This condition is automatically satisfied because the damping coefficient d is positive. In the special case of an undamped system, $\xi = 0$, the roots of the polynomial equation may lie on the imaginary axis and the system may be marginally stable if all other conditions in Eq. (31) are satisfied.
- The second and the third inequalities in Eq. (31) require that α_{01} and α_{02} be positive. From Eqs. (19), we see that these terms consist of the plate aspect ratio, the fluid/structure density ratio, and the added mass due to acoustic radiation. All these quantities are positive. Therefore these two conditions are satisfied automatically.

- The last two inequalities in Eq. (31) require both Γ_1 and Γ_2 to be positive. Substituting the plate's undeformed equilibrium position given by Eq. (23a) into (29), we have $\Gamma_1 = \alpha_1$ and $\Gamma_2 = \alpha_2$. The quantities $\alpha_{1,2}$ represent the effect of the stiffness and that of the added stiffness due to acoustic radiation in the presence of mean flow [see Eqs. (19c) and (19d)], respectively. The former is positive, but the latter is negative, because $\Theta^{(2)}_{1111}$ and $\Theta^{(2)}_{2121}$ are negative [see Eq. (17d)]. Without mean flow, the added stiffness is identically zero. Hence α_1 and α_2 are always positive, which means $\Gamma_1 > 0$ and $\Gamma_2 > 0$ and the plate is stable around its undeformed equilibrium position. When there is mean flow and when the mean flow speed is low, the effect of the added stiffness is small. Therefore α_1 and α_2 are positive, and the plate is still stable. However, the values of α_1 and α_2 decrease with the increase of the mean flow speed. When the mean flow speed exceeds certain critical value such that the added stiffness overwhelms the plate stiffness, then α_1 or α_2 may be negative and the plate may become locally unstable.

- The quantities α_1 and α_2 decrease quadratically with the mean flow speed [see Eqs. (19c) and (19d)]. Hence, the higher the mean flow speed, the more unstable the plate may be.

- The plate aspect ratio and the plate's length/thickness ratio have a direct effect on the overall stiffness. The larger the plate aspect ratio and the plate's length/thickness ratio, the smaller the plate overall stiffness, and the more unstable the plate tends to be.

- The critical mean flow speed can be determined by setting Γ_1 and Γ_2 to zero, which is equivalent to setting α_1 and α_2 to zero. From Eqs. (19c) and (19d), we obtain

$$u_{cr,1} = \sqrt{-\frac{2\pi D}{\rho_0 \eta L^3 \Theta^{(2)}_{2121}} \left(\lambda_2^4 + 2\frac{\theta_{11}\theta_{22}}{\eta^2} + \frac{\lambda_1^4}{\eta^4} \right)}. \tag{32a}$$

$$u_{cr,2} = \sqrt{-\frac{2\pi D}{\rho_0 \eta L^3 \Theta^{(2)}_{1111}} \left(\lambda_1^4 + 2\frac{\theta_{11}^2}{\eta^2} + \frac{\lambda_1^4}{\eta^4} \right)}, \tag{32b}$$

  - Suppose that $u_{cr,1} < u_{cr,2}$. Then if $U = u_{cr,1}$, we have $\alpha_1 > 0$ and $\alpha_2 = 0$. In this case the equilibrium position still remains unchanged, but $\Gamma_1 = \alpha_1 > 0$ and $\Gamma_2 = \alpha_2 = 0$. The last inequality in Eq. (31) is not satisfied. So the plate at its original equilibrium position may start to become locally unstable.

  - When $u_{cr,1} < U < u_{cr,2}$, then $\alpha_1 > 0$ and $\alpha_2 < 0$. In this case, a new equilibrium position given by Eq. (23c) emerges in addition to the original undeformed one. However, the plate at the original equilibrium position may by locally unstable because $\Gamma_1 = \alpha_1 > 0$ and $\Gamma_2 = \alpha < 0$, while stable at the new equilibrium position since $\Gamma_1 = \alpha_1 - \alpha_2\alpha_5/\alpha_6 > 0$ and $\Gamma_2 = -2\alpha_2 > 0$.

  - When $U = u_{cr,2}$, we have $\alpha_1 = 0$ and $\alpha_2 < 0$. In this case, the equilibrium position given by Eq. (23c) co-exists with the original undeformed equilibrium position. Once again, the plate may be locally unstable at the original equilibrium position because $\Gamma_1 = \alpha_1 = 0$ and $\Gamma_2 = \alpha_2 < 0$, but stable at the new equilibrium position since $\Gamma_1 = -\alpha_2\alpha_5/\alpha_6 > 0$ and $\Gamma_2 = -2\alpha_2 > 0$.

- When the mean flow speed exceeds both critical values, $U > u_{cr,1}$ and $U > u_{cr,2}$, then both α_1 and α_2 will be negative. In this case, there may be up to four equilibrium positions given by Eqs. (23). However, Γ_1 and Γ_2 cannot be positive simultaneously at all of these equilibrium positions. Therefore the plate may be locally unstable everywhere.

- The local instabilities are controlled by the structural nonlinearities. Without the inclusion of structural nonlinearities, there is only one equilibrium position, i.e., the undeformed flat position. Under this condition, the amplitude of plate vibration would grow exponentially in time when the mean flow speed exceeds the critical values, known as absolute instability. With the inclusion of the structural nonlinearities, the overall amplitude of vibration is bounded. However, plate vibration may be locally unstable, jumping from one equilibrium position to another. In particular, this jumping may be random and plate vibration may seem to be chaotic.

5. NUMERICAL EXAMPLES

In the preceding section, we have seen that a finite, baffled elastic plate may become locally unstable when there is mean flow. The instabilities occur whenever the overall stiffness becomes negative. In this section, we show numerical results of a finite, baffled elastic plate in the presence of mean flow. In particular, we demonstrate transition of plate vibration from stable to locally unstable as the mean flow speed increases.

First, we define the dimensionless critical mean flow speed. From Eqs. (16b) and (32), we have

$$\zeta_{cr,1} = \sqrt{-\frac{2\pi}{\eta\Theta^{(2)}_{2121}}\left(\lambda_2^4 + 2\frac{\theta_{11}\theta_{22}}{\eta^2} + \frac{\lambda_1^4}{\eta^4}\right)}, \tag{33a}$$

$$\zeta_{cr,2} = \sqrt{-\frac{2\pi}{\eta\Theta^{(2)}_{1111}}\left(\lambda_1^4 + 2\frac{\theta_{11}^2}{\eta^2} + \frac{\lambda_1^4}{\eta^4}\right)}, \tag{33b}$$

Similarly, the dimensionless mean flow speed can be written as

$$\zeta = \sqrt{\frac{\rho_0 L^3 U^2}{D}} = M\left(\frac{c}{c_p}\right)\sqrt{12\left(\frac{\rho_0}{\rho}\right)\left(\frac{L}{h}\right)^3}, \tag{34}$$

where $c_p = \sqrt{E/\rho_p/(1-\nu^2)}$ is the compressional wave speed of the plate, [15] and the commonly accepted value of c_p for a steel plate is 5400 (m/s)

As an example, we consider a steel plate in contact with water on one side and vacuum on the other side. The plate has a density $\rho_p = 7800$ (kg/m^3), a length $L = 2.5$ (m), a width $b = 1.25$ (m), and a thickness $h = 0.003$ (m). Accordingly, the plate aspect ratio $\eta = 0.5$, the plate length/thickness ratio $L/h = 833.3$, the fluid/structure density ratio $\mu = 106.84$, and the dimensionless mean flow speed $\zeta = 8288.36M$. For most engineering applications, the mean flow Mach number M is typically in the range of 0 to 0.01. The critical dimensionless mean flow speeds are found to be $\zeta_{cr,1} = 57.97$ and $\zeta_{cr,2} = 74.23$

based on Eqs. (33). The clamped plate is assumed to have an initial displacement with $\bar{Y}_1(0) = \bar{Y}_3(0) = 0.05$ and $\bar{Y}_2(0) = \bar{Y}_4(0) = 0$. As in all nonlinear systems, the responses are sensitive to the initial conditions. The set of initial conditions selected above has been found to be one of the best to depict local instabilities as the mean flow speed increases.

The plate flexural displacement is obtained by solving a set of NODEs (21) using the Gear's method.[16] Figure 1 shows the amplitude of dimensionless displacement at $\bar{x} = 0.75$ and $\bar{y} = 0.5$ versus dimensionless time $\bar{t}$, with a zero damping ratio $\xi = 0$, and a dimensionless mean flow speed $\zeta = 41.44$. Since $\zeta < \zeta_{cr,1}$ and $\zeta_{cr,2}$, the plate is stable around its original undeformed equilibrium position. Numerical results show that two longitudinal modes are coupled together and the effect of structural nonlinearities is obvious. Next, we increase the dimensionless mean flow speed to $\zeta = 66.31$. Since $\zeta_{cr,1} < \zeta < \zeta_{cr,2}$, the plate becomes locally unstable around its original equilibrium position, and nevertheless stable around a new equilibrium position (see Fig. 2). Finally, we set the dimensionless mean flow speed at $\zeta = 82.88$, which is larger than both $\zeta_{cr,1}$ and $\zeta_{cr,2}$. Under this condition, the plate has three equilibrium positions, but none of them are unstable. In particular, plate vibration is observed to jump from one equilibrium position to another. Since this jump is completely random, plate vibration seems to be totally chaotic (see Fig. 3).

6. CONCLUSIONS

The mechanism of local instabilities of a finite, elastic plate can be attributable to the added stiffness induced by acoustic radiation in mean flow. When there is no mean flow, the stiffness is positive and the plate is always stable around its undeformed equilibrium position. When there is mean flow and when the mean flow speed is very low, the effect of added stiffness due to acoustic radiation in mean flow is small and the plate overall stiffness is positive. Hence the plate is still stable. However, the added stiffness increases quadratically with the mean flow speed. When the mean flow speed is large enough so that the overall stiffness becomes negative, then the plate may be locally unstable around its original undeformed equilibrium position, and stable at a different equilibrium position. When the mean flow speed exceeds all the critical values, plate vibration may become locally unstable at all equilibrium positions. In particular, plate vibration may jump from one equilibrium position to another. Since this jump is completely random, plate vibration may seem to be totally chaotic.

The local instabilities described above are controlled by structural nonlinearities. Without the inclusion of structural nonlinearities, the plate may have only one equilibrium position, i.e., its undeformed one. The amplitude of plate vibration would then grow unboundedly in time when the mean flow speed exceeds a critical value, known as absolute instability. With the inclusion of structural nonlinearities, the plate may have more than one equilibrium positions when the mean flow speed exceeds the critical ones. As a result, plate vibration may jump from one equilibrium position to another. The amplitude of plate vibration, nevertheless, is bounded.

ACKNOWLEDGMENTS

The work was supported by the Office of Naval Research Grant No. N00014-89-J-3138.

REFERENCES

1 Dowell, E. H., Flutter of infinitely long plates and shells—Part I: Plate, JOURNAL OF THE AMERICAN INSTITUTE OF AERONAUTICS AND ASTRONAUTICS, 4 (1966), 1370 – 1377.

2 Dowell, E. H., Nonlinear oscillations of a fluttering plate. II, JOURNAL OF THE AMERICAN INSTITUTE OF AERONAUTICS AND ASTRONAUTICS, 5 (1967), 1856 – 1862.

3 E. H. Dowell, Flutter of a buckled plate as an example of chaotic motion of a deterministic autonomous system, AEROELASTICITY OF PLATES AND SHELLS, The Netherlands: Noordhoff International Publishing, Leyden, 1974.

4 Ellen, C. H., Stability of clamped rectangular plates in uniform subsonic flow, JOURNAL OF THE AMERICAN INSTITUTE OF AERONAUTICS AND ASTRONAUTICS, 10 (1972), 1716 – 1717.

5 Ellen, C. H., The stability of simply supported rectangular surfaces in uniform subsonic flow, JOURNAL OF APPLIED MECHANICS, 40 (1973), 68 – 72.

6 Kornecki, A., Dowell, E. H. Dowell, and O'Brien, J., On the aeroelastic instability of two-dimensional panels in uniform incompressible flow, JOURNAL OF SOUND AND VIBRATION, 47 (1976), 163 – 178.

7 Brazier-Smith, P. R., and Scott, J. F., Stability of fluid flow in the presence of a complaint surface, WAVE MOTION, 6 (1984), 547 – 560.

8 Crighton, D. C., and Oswell, J. E., Fluid loading with mean flow. I. Response of an elastic plate to localized excitation, PHILOSOPHICAL TRANSACTIONS OF THE ROYAL SOCIETY OF LONDON, 335 (1991), 557 – 592.

9 Leissa, A. W., Vibration of plates, NASA, SCIENTIFIC INFORMATION DIVISION, Washington, D.C., 1969.

10 Pierce, A. D., Acoustics: An introduction to its physical principles and applications, MCGRAW-HILLS, New York, 1981.

11 Wu, S. F. and Maestrello, L., Responses of finite baffled plate to turbulent flow excitation, JOURNAL OF THE AMERICAN INSTITUTE OF AERONAUTICS AND ASTRONAUTICS, 33 (1995), 13 – 19.

12 Zhu, J., Acoustic and dynamic responses of fluid-loaded plates in mean flow, PH.D DISSERTATION, WAYNE STATE UNIVERSITY, DETROIT, MICHIGAN, 1995.

13 Guckenheimer, J., and Homes, P., Nonlinear Oscillations, Dynamical Systems, and Bifurcations of Vector Fields, SPRINGER-VERLAG, New York, 1983.

14 Ogata, K., Modern Control Engineering, PRENTICE-HALL, New Jersey, 1970.

15 Junger, M. G., and Feit, D., Sound, structures and their interaction, CAMBRIDGE, MASSACHUSETTS: MIT PRESS, 1972.

16 Gear, C. W., Numerical initial-value problems in ordinary differential equations, PRENTICE-HALL, ENGLEWOOD CLIFFS, NEW JERSEY, 1971.

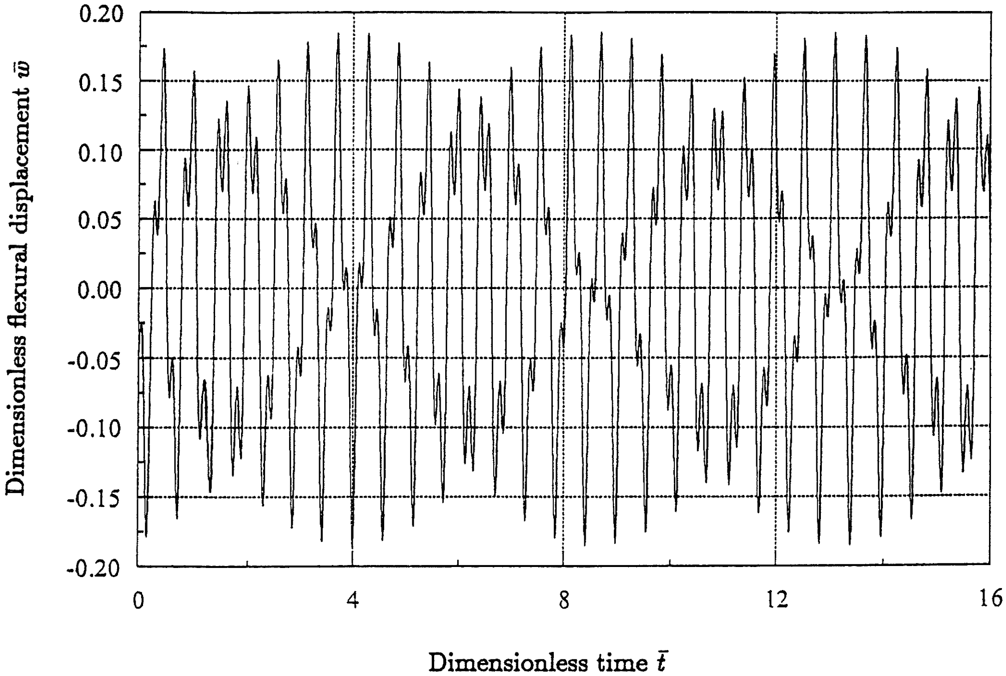

Figure 1. Plate vibration responses at $\zeta = 41.44$ ($\zeta < \zeta_{cr,1}$ and $\zeta < \zeta_{cr,2}$).

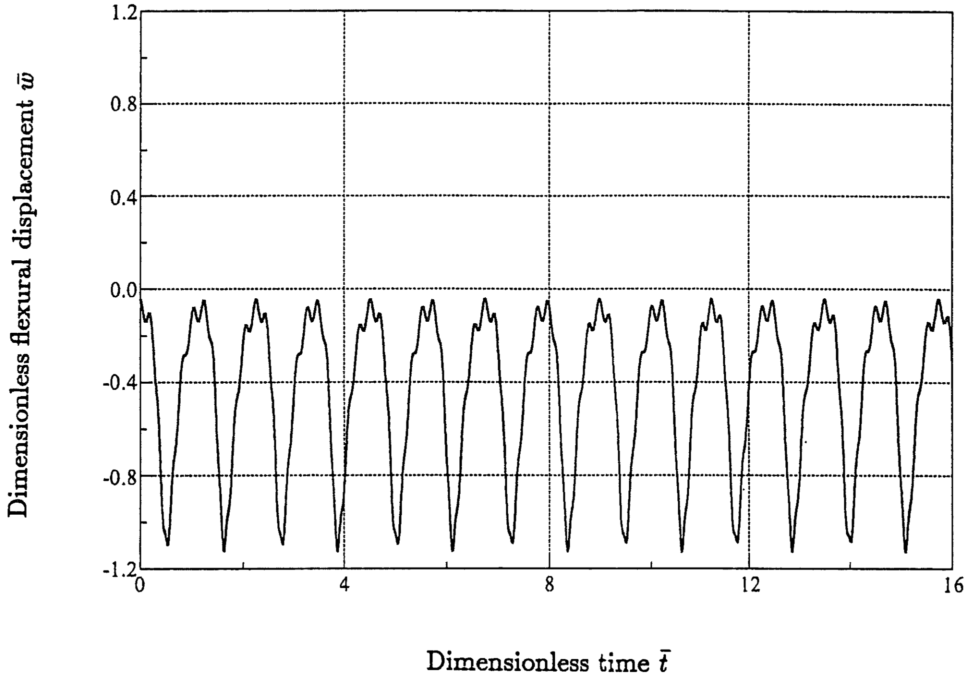

Figure 2. Plate vibration responses at $\zeta = 66.31$ ($\zeta_{cr,1} < \zeta < \zeta_{cr,2}$).

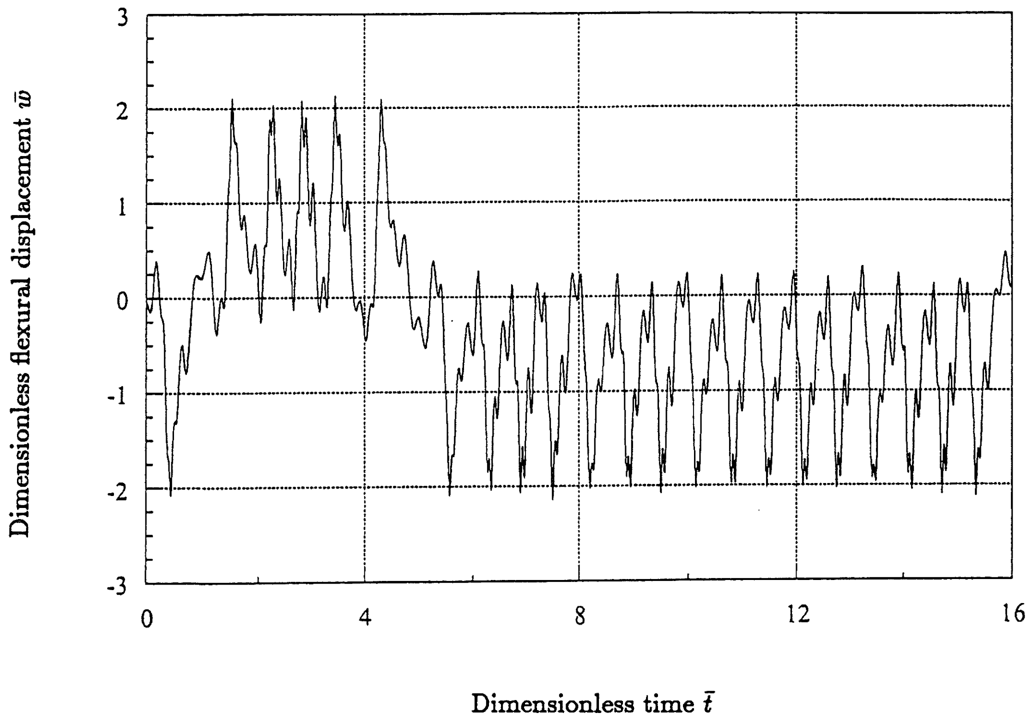

Figure 3. Plate vibration responses at $\zeta = 82.88$ ($\zeta > \zeta_{cr,1}$ and $\zeta > \zeta_{cr,2}$).